Supporting materials

Text S1: Analytical methods

Before measurement, the Pt electrode was rinsed with water to remove electrolyte and dried in the air. Fourier transformed infrared (FTIR) spectra was obtained using on Infrared Spectrometer (Prestige-21, Shimadzu, Japan). The interferograms were acquired with the Pt working electrode surface pressed against this window and were collected at 4 cm^{-1} resolution. The chemical compositions of Pt electrode before and after reaction were characterized by using an X-ray photoelectron spectroscopy (XPS) (PHI-5700, ULVCA-PHI, Japan). All binding energies were calibrated with surface adventitious carbon of 284.6 eV. The generated radicals trapped with 5, 5-dimethyl-1-pyrroline N-oxide (DMPO, Aladdin Reagent Company, China) in the process of electrochemical oxidation reaction was detected by electron spin-resonance spectroscopy (ESR, Bruker, Germany). All experiments were performed at room temperature.

Text S2: Measurements of the electrochemically active surface areas (ECSA) of pristine and fouled Pt electrode

We used hydrogen adsorption-desorption on Pt electrode in acidic condition to measure the ECSA. The tests were conducted using 0.5 M of sulfuric acid (H_2SO_4, Tianjin Kermel Chemical Reagent Co. Ltd, China) aqueous solution that was purged with argon for about 30 min. The cyclic voltammetry (CV) was recorded between 0.0 and 1.0 V vs. SHE with a scan rate of 0.1 V/s. The ECSA was derived from the area under a backward potential curve between 0.05 V and 0.40 V, the region accounting for hydrogen adsorption (Lee et al., 2007) as

$$C = \int_{t_0}^{t_1} I dt = \int_{0.05}^{0.40} \frac{I \times dE}{v} , \qquad \text{(S1)}$$

$$ECSA = \frac{C}{Q} , \qquad \text{(S2)}$$

where C (C, unit) is the charge, I (A, unit) the current, E (V vs SHE) the potential, v (V/s) the scan rate, and Q (C/cm^2, unit) the charge density during the hydrogen adsorption. The value of Q used for ECSA calculation was experimentally determined to be 210 μC/cm^2 for a Pt surface, which represented the maximum hydrogen adsorbed, and was close to the average value expected for the full coverage of close-packed Pt surface (Parthasarathy et al., 1992).

Text S3: Calculation of the Pt electrode mass change using the EQCM by Sauerbrey equation

A Model QCA 922 electrochemical quartz crystal microbalance (EQCM) and a Model 263A potentiostat-galvanostat used for this study of the mass change of electrode. A Keithley 500 series analogto-digital converter was connected to a personal computer and used for data acquisition, including the electrode potential, the electrode current and the quartz crystal frequency change obtained with the EQCM apparatus. The working electrode (WE) was 9 MHz AT-cut Pt quartz crystal with a geometric area of 0.196 cm^2, which was immobilized on the bottom of the electrochemical cell by silicone rubber adhesive. A platinum wire and Ag/AgCl were used as counter electrode (CE) and reference electrode (RE), respectively, in a separate compartment connected to the main electrolyte. The schematic of electrochemical cell using EQCM measurement was shown in Fig. S1.

EQCM is composed with a thin piezoelectric quartz crystal sandwiched between two metal electrodes used to create an alternating electric field across the crystal, causing vibrational motion of the crystal at its resonance frequency. The shift of the quartz resonance frequency (Δf) can be converted into mass change (Δm) on the quartz crystal and electrodes by applying Sauerbrey's equation (Tuna et al., 2019):

$$\Delta m = -\frac{\Delta f A\sqrt{\rho_q \mu_q}}{2nf_0^2}, \qquad \text{(S3)}$$

where Δm is the change in mass, Δf is the change in resonant frequency of the quartz crystal, A is the area of working electrode (0.196 cm^2), ρ_q is the density of quartz (2.648 $\mathrm{g/cm}^3$), μ_q is the shear modulus of quartz (2.947×10^{11} $\mathrm{g/cm/s}^2$), n is the number of harmonic at which the crystal is driven (set to 1 by design), and f_0 is the resonant frequency of the fundamental mode of the loaded crystal (9 MHz). It should be noted that the Sauerbrey equation as described above assumes an atomically flat and rigid electrode surface.

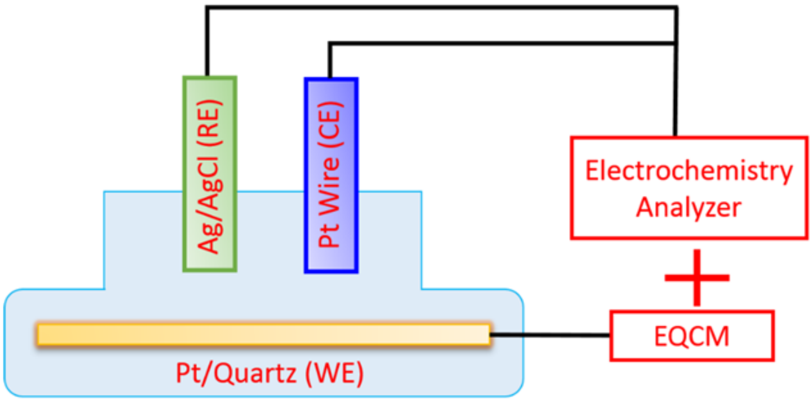

Fig. S1 Schematic illustration of electrochemical cell for measuring mass change of Pt electrode by using EQCM

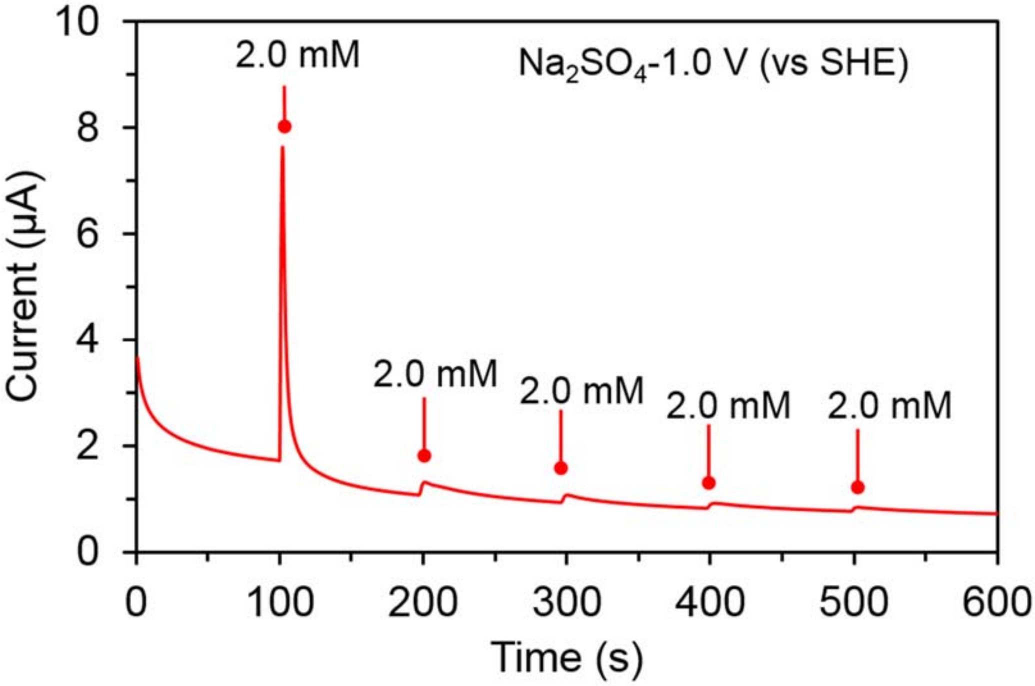

Fig. S2 Chronoamperometric response of Pt electrode to step-by-step injection of phenol in 0.1 M Na_2SO_4 (pH 6.8 ± 0.5) at 1.0 V vs SHE

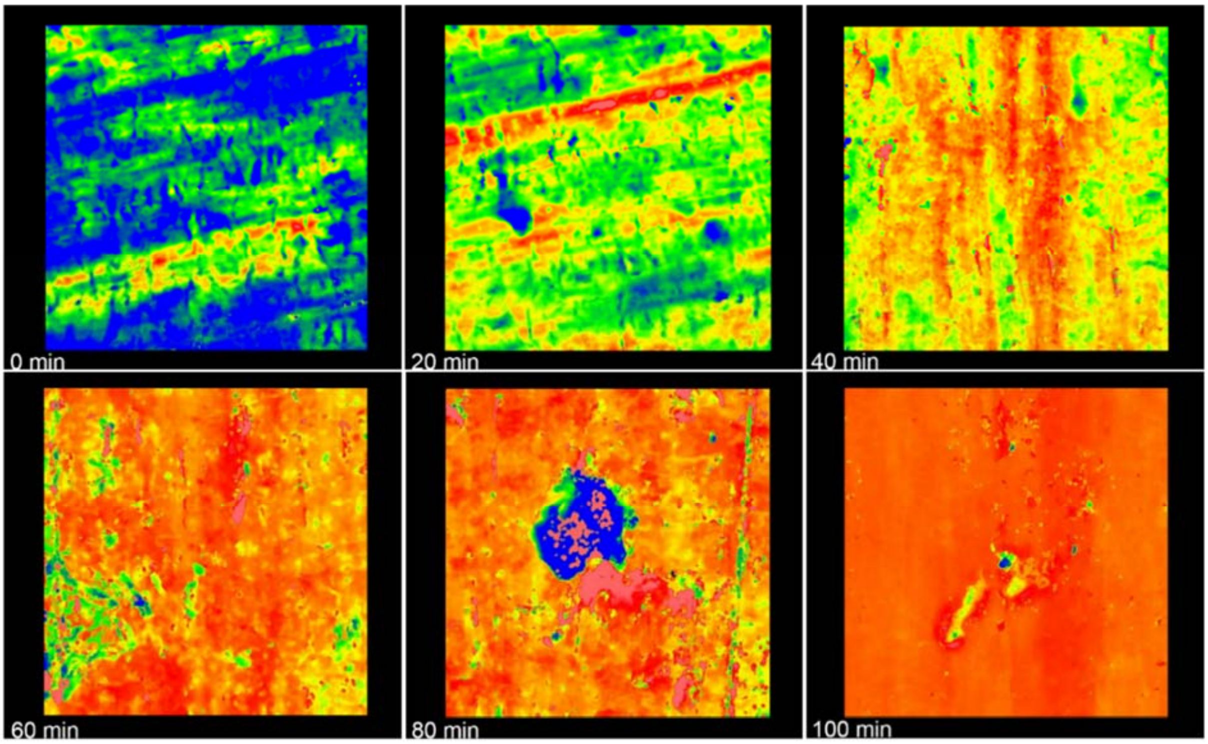

Fig. S3 The surface images of Pt electrode during electrolysis of 2.0 mM phenol in 0.1 M NaCl at 1.0 V vs SHE

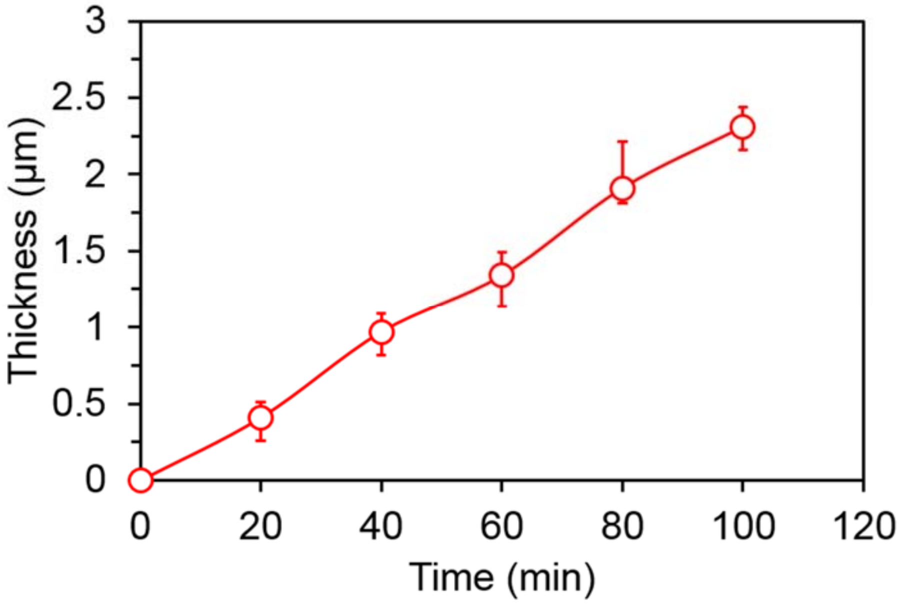

Fig. S4 The thickness fouling film formed on Pt electrode during electrolysis

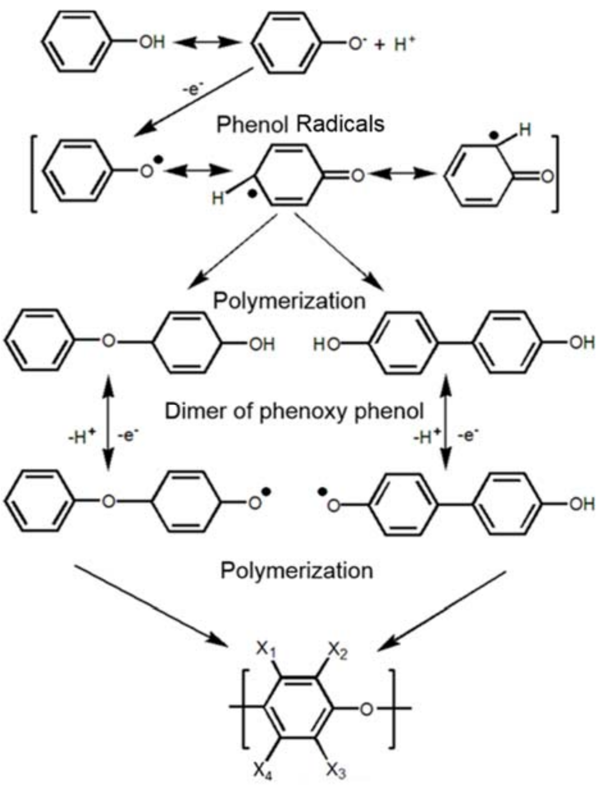

Fig. S5 Schematic representation of the pathway for the formation of fouling film during the anodic oxidation of phenol where X = hydrogen, substituent group or adjacent ring

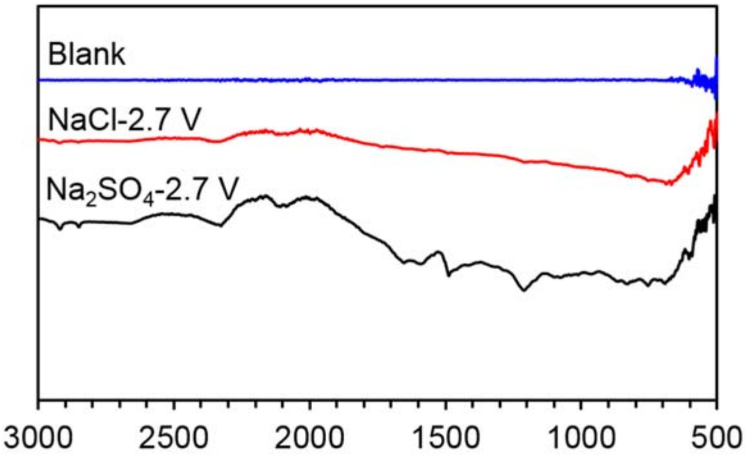

Fig. S6 FTIR spectras during electrolysis of 2.0 mM phenol in 0.1 M NaCl or Na$_2$SO$_4$ at 2.7 V vs SHE within 100 min

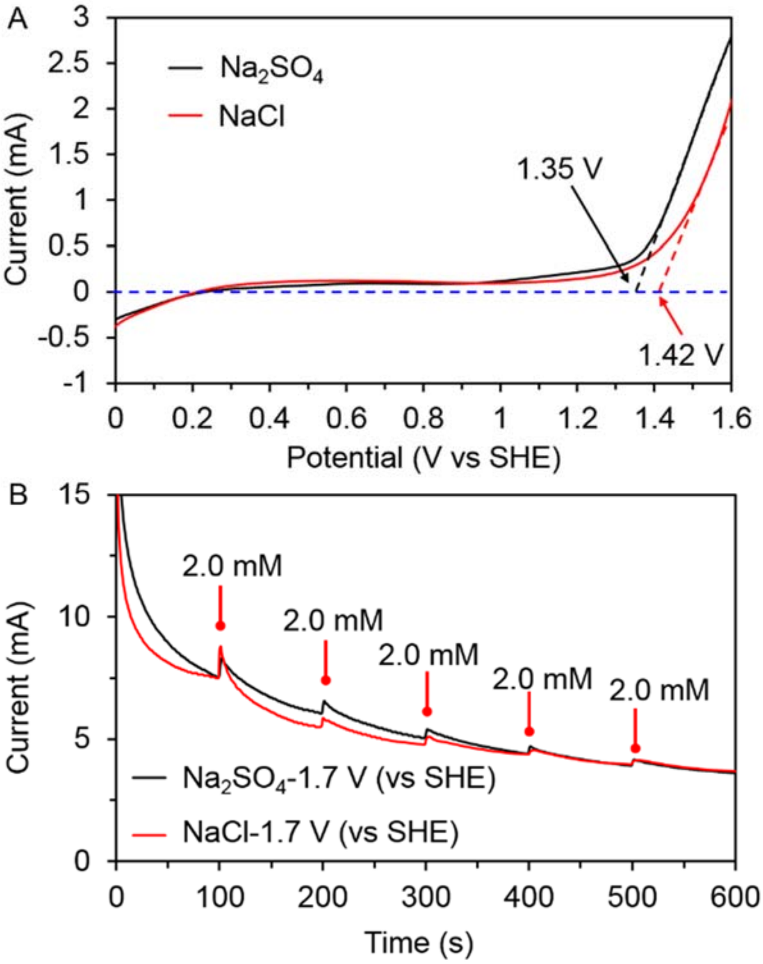

Fig. S7 (a) LSV curves of Pt electrode in 0.1 M Na$_2$SO$_4$ and 0.1 M NaCl at scan rate of 10 mV/s and (b) chronoamperometric response of Pt electrode to step-by-step injection of phenol at 1.7 V vs SHE in 0.1 M NaCl or 0.1 M Na$_2$SO$_4$

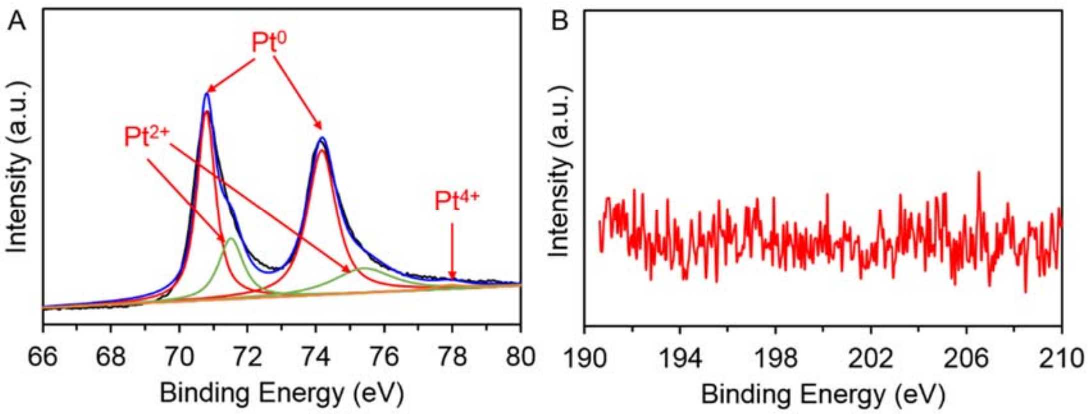

Fig. S8 High-resolution XPS spectra of (a) fouled Pt anode and (b) Cl2p after electrolysis of 2.0 mM phenol in 0.1 M Na_2SO_4 electrolyte at 2.7 V vs SHE

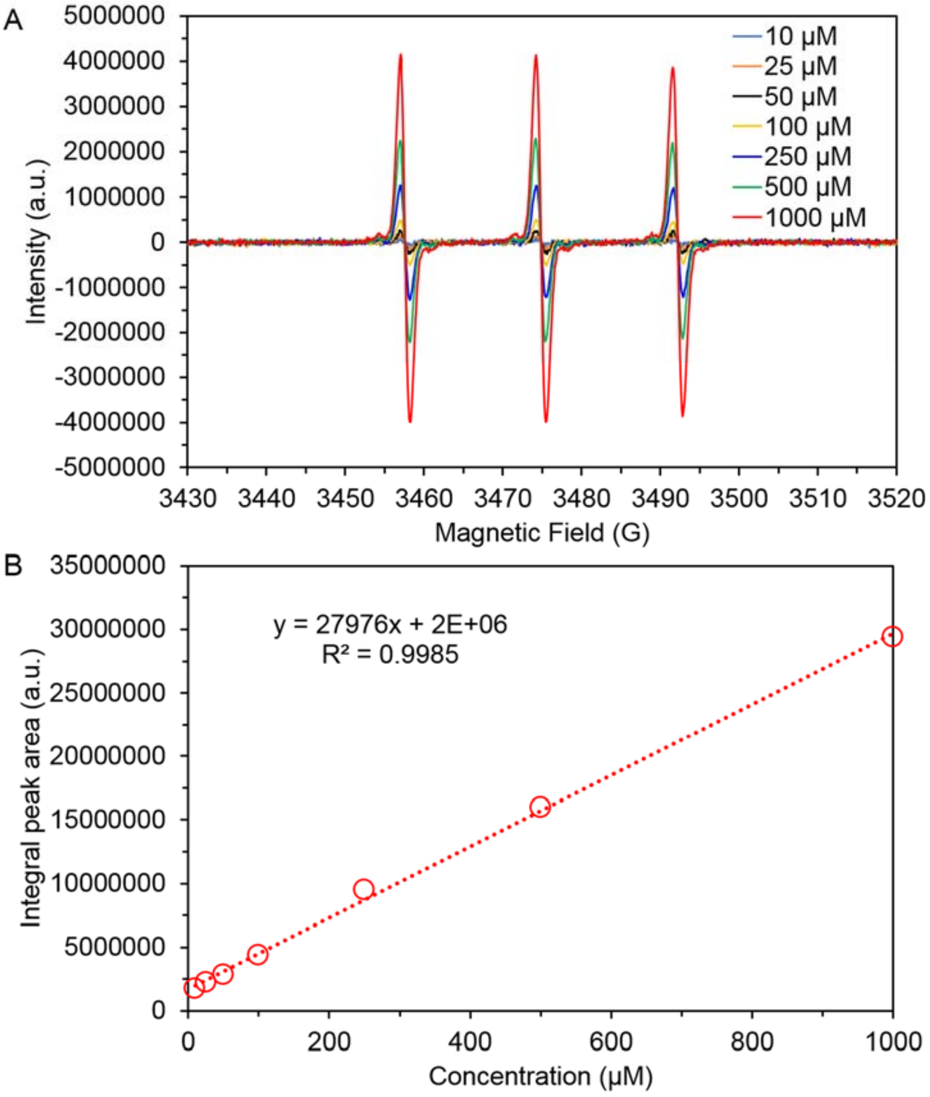

Fig. S9 (a) ESR spectra of TEMPOL and (b) The standard curves of TEMPOL concentration versus integral peak area derived from ESR data

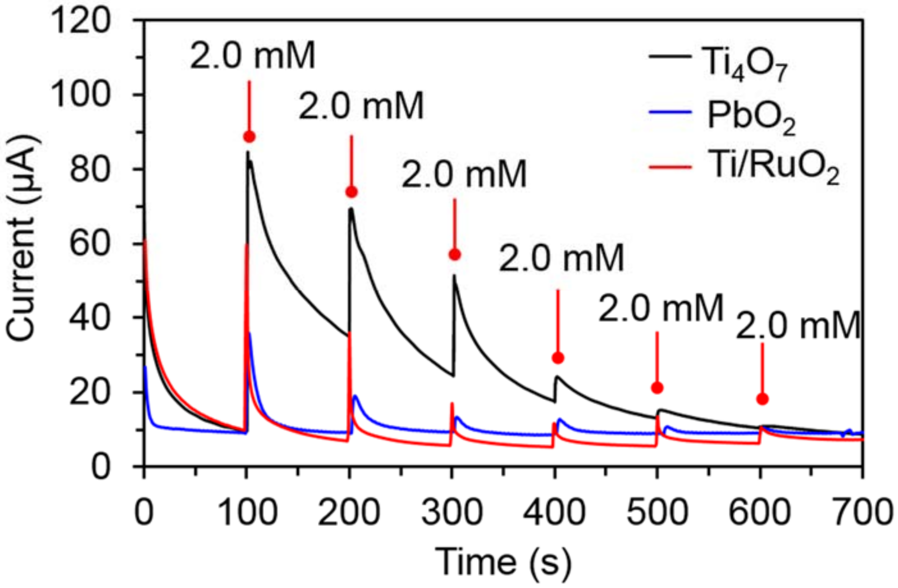

Fig. S10 Chronoamperometric response of Ti_4O_7, PbO_2 and Ti/RuO_2 electrodes to step-by-step injection of phenol in 0.1 M NaCl (pH 6.8 ± 0.5) at 1.0 V vs SHE

References

Lee E P, Peng Z M, Cate D M, Yang H, Campbell C T, Xia Y N (2007). Growing Pt nanowires as a densely packed array on metal gauze. Journal of the American Chemical Society, 129(35): 10634–10635 doi:10.1021/ja074312e

Parthasarathy A, Srinivasan S, Appleby A J, Martin C R (1992). Temperature dependence of the electrode kinetics of oxygen reduction at the Platinum/Nafion® interfaces: A microelectrode investigation. Journal of the Electrochemical Society, 139: 2530–2537 doi:10.1149/1.2221258

Tuna K, Kilian A, Ressler T (2019). EQCM and EIS characterization of electrochemical deposition of tin from aqueous solution containing pyrophosphate. Electrochimica Acta, 296: 224–234